Size distributions, scaling properties, and Bartelt-Evans singularities in irreversible growth with size-dependent capture coefficients

V. G. Dubrovskii[1,2,3,*] and N. V. Sibirev[1,3]

[1]*St. Petersburg Academic University, Khlopina 8/3, 194021 St. Petersburg, Russia*

[2]*Ioffe Physical Technical Institute of the Russian Academy of Sciences, Politekhnicheskaya 26, 194021 St. Petersburg, Russia*

[3]*St. Petersburg State University (Physical Faculty), Ulianovskaya Street 3, Petrodvorets, 198504 St. Petersburg, Russia*

(Received 29 October 2013; revised manuscript received 6 January 2014; published 20 February 2014)

We present a theoretical analysis of the rate equations for irreversible growth with a monomer influx, desorption, and a power-law dependence of the capture coefficients on the number of monomers s. Special emphasis is given to the size distribution shapes and their time invariance in terms of a new variable which is distinctly different from the conventional s/s_* ratio, with s_* being a representative size in the distribution. Our results can be briefly formulated as follows. First, we generalize the earlier results to systems with desorption. Second, the analytical size distributions are obtained by applying the transformation to a certain invariant size variable (ρ) for which the regular growth rate is independent of the cluster size, and the Green function in the form of Gaussian with a spreading dispersion. Third, the size distribution shapes reflect the time dependence of the monomer concentration inverted in terms of the $z-\rho$ variable, with z as a representative invariant size. Fourth, the fluctuation-induced broadening of these spectra depends critically on the growth law. Fifth, the obtained distributions show a refined time-invariant scaling in the appropriate variables for a broad range of conditions and for all but very small z, while the scaling in terms of ρ/z works only in the formal limit $z \to \infty$.

DOI: 10.1103/PhysRevB.89.054305 PACS number(s): 64.60.Q−

I. INTRODUCTION

There has been large interest in theoretical modeling of the diffusion-induced irreversible growth in open systems, particularly in connection with size distributions (SDs) of two-dimensional (2D) surface islands during vapor deposition at a low coverage [1–22]. These studies are essential for understanding general properties of irreversible aggregations and maintaining the necessary control over the island morphology. It should be noted that similar growth models apply also to three-dimensional (3D) systems, for example, liquid droplets in supersaturated vapor surroundings (such as catalyst droplets during the vapor-liquid-solid growth of nanowires [23]) or one-dimensional (1D) polymer chains in 3D liquid solutions [24]. The most straightforward way to obtain the time-dependent SDs of "clusters" is applying the mean field rate equations (REs) [1–3,5,9,10,12–14,16–24] with a monomer influx (vapor flux for 2D islands) and sink (desorption) and certain "capture coefficients" which depend on the mechanism of material transport into the clusters. This approach should work well at a low temperature and coverage, where the growing clusters are terminated by distinct boundaries and do not coalesce. Of course, the mean field treatment fails when subtle correlations between island size and separation affect the effective capture coefficients and thus control the SD shapes [7,18].

The core assumption of irreversible growth models is the effective absence of cluster decay. Strictly speaking, there are no physical systems without decay since it is against thermodynamics. Indeed, the growth and evaporation rate constants should be related to each other through the detailed balance involving the cluster formation energy, as usual in general nucleation theory [23,25–35]. This brings about the notions of supersaturation, the supersaturation-dependent critical size, the nucleation barrier, and the Zeldovich nucleation rate which is extremely sensitive to supersaturation. The entire growth process can be divided into distinctly different steps (see Ref. [36] for the review in the case of crystal growth far from equilibrium), separated due to a timescale hierarchy. One can distinguish the nucleation stage [23,25–31], the regular growth stage [23,30,32], and the Ostwald ripening [33], where the nucleation stage is the shortest under a material influx [23,26–28,31]. Therefore, the assumption of irreversible growth can apply only within a certain interval of time and relates to the case of very high supersaturation, with the critical size close to one [3]. As supersaturation drops down, the critical size starts increasing, the Zeldovich nucleation rate rapidly tends to zero so that further nucleation is disabled. When decay is neglected, the monomer concentration tends to zero rather than to a certain equilibrium value, while clusters of all sizes always continue growing [5,6,15–22].

This fundamental difference leads to rather dissimilar SD shapes. In nucleation theory with decay, the SDs are more or less symmetrical (Gaussian) around their most representative size and rapidly decreasing for both large and small sizes [23,26,27,31,32,34,35], while they feature a very long left tail in irreversible growth models [5–10,17,18]. Without desorption, the scaled SD does not even vanish for small sizes [6,18]. In this respect, the assumption of no decay in the REs for irreversible growth should be considered much less justified than the mean field RE approach itself and can hardly work in the large time limit. On the other hand, it can be well applied for systems with very high diffusivity but for modest growth times, where many-particle correlation effects can be neglected. Here, one of the most interesting features of the SDs discussed in the literature is the so-called scaling properties [4,5,6,12,15,17]. This scaling has an important impact on

*Corresponding author: dubrovskii@mail.ioffe.ru

the asymptotic spectrum shapes and even on the activation energies of elementary processes on solid surfaces [37].

There are several formulations of scaling in irreversible growth of 2D surface islands given, e.g. by Vicsek and Family [4] and then developed by Korner *et al*. [17], or those considered by Bartelt and Evans [5,6]. With neglect of desorption and at a low coverage, the Bartelt-Evans formulation [5] can be put as follows. In the limit of large ratios of diffusion constant over deposition rate, the ratio of the SD (f_s) to the concentration of free monomers (f_1) is expected to be a unique function of the ratio s/s_*, where s_* is the representative size in the SD (say, proportional to the average size $\langle s\rangle$: $s_* = B\langle s\rangle$, with B independent of time), for all but short times: $f_s/f_1 = \varphi(s/s_*)$. More generally, scaling can be searched for in the form $(f_s/\nu^{1/2})s_*^{\eta} = \varphi(s/s_*)$, with a certain power index η and ν being proportional to the diffusion coefficient D [6,17]. Another equivalent formulation [4,5,15] states that $f_s = [G/s_*^2]\varphi(s/s_*)$, where G is the surface coverage. It has been shown then that, in the case of size-independent capture coefficients, the irreversible growth model yields a mathematical singularity of the SDs in terms of such scaling variables [5]. This result follows from the corresponding REs and is supported by kinetic Monte Carlo simulations. Subsequent work, summarized, for example, in the review paper [18], suggested that breaking the scaling property is the fundamental drawback of the model with size-independent capture coefficients, which is why it is unable to qualitatively reproduce the SDs. According to this view, only the correct account for both the size and the coverage dependence of the capture coefficients allow for the adequate description of the SDs with REs.

In this paper, we address several fundamental properties of the SDs described within REs for irreversible growth with desorption and at a low coverage. In the case of surface islands, desorption sets a limitation on the adatom diffusion length [23], which may disable competition for the diffusion fluxes and thus better justify the mean field approach at an early growth stage. Our analysis of the REs is based on the approach developed earlier in general nucleation theory with decay of clusters [23,26–28,30–32] which, to the best of our knowledge, has not been used in the irreversible growth models so far. Compared to the analytical and numerical methods treating the island SD $f_s(t)$ as a function of the "natural variables" s, t and then searching the time-invariant solutions in the form $f_s(t) = \nu^{1/2}s_*^{-\eta}\varphi(s/s_*)$ (usually with neglect of desorption) [5,15,18,22], our approach is based on a special transformation of variables [23]. Following Kuni [26], we eliminate the nonlinearity of the REs caused by the time dependence of the monomer concentration and then get rid of the SD deformation due to the size dependence of the capture coefficients. This allows one to use the Green function method [30–32] and to find a refined scaling which gives a more detailed picture of the SD behavior under different conditions. This scaling does not require the assumptions of high diffusivity and no desorption.

The paper is organized as follows. Section II presents the basic REs in the form which is most convenient for further analyses. In Sec. III, we reconsider the irreversible growth model with size-independent capture coefficients, for which the exact solution is easily obtained for the discrete REs [5] also when desorption is included. We show that the continuum (large size) asymptote of this solution is a time-invariant (or "scaling") function of a variable which is distinctly different from s/s_* or $s/\langle s\rangle$. When plotted in the s/s_* variable, the solution features the Bartelt-Evans singularity in the large time limit or for high diffusivity, showing simply that such a representation is not time-invariant for all s. However, scaling in terms of s/s_* holds for the long left tail of the SDs at small enough s, i.e. for most clusters except those near the distribution maximum and on an abrupt right tail. In Sec. IV, we consider 1D, 2D, and 3D clusters (linear chains, nanowires, islands, and droplets) in 2D and 3D environments and show that the relevant size dependence of the capture coefficients in the continuum limit ($s \gg 1$) has the power law form $s^{(m-1)/m}$ [15,23], with the growth index m ranging typically from 1 to 3.

Section V presents the analytical solutions to the continuum RE with a power law size dependence of the capture coefficients, based on the linearization of the RE, the transformation to the so-called invariant SD g_s [23,26–32] and the Green function method [30–32]. It is shown that the obtained continuum solutions immediately yield the universal, time-invariant shapes of the SDs which depend only on the growth index m. This behavior follows from the mathematical properties of the continuum REs. Namely, the time invariance is preserved in terms of the variables $g_s/\nu^{1/2}$ and $s_*^{1/m} - s^{1/m}$ for $m \geqslant 2$ or $(g_s/\nu^{1/2})s_*^{\eta}$ and $(s_*^{1/m} - s^{1/m})/s_*^{1/m-1/2}$ for $m < 2$, depending on whether kinetic fluctuations are effective or not. When fluctuations broaden the SDs, the power exponent η is different from that of $1/f_1$ due to this broadening. In Sec. VI, the asymptotic solutions for the monomer concentration, cluster density, average size, and ultimately the SDs are obtained in complete condensation regime for different m. Finally, the analysis of Sec. VII shows that the time-invariant scaling in terms of the s/s_* variable is generally broken regardless of the particular size dependence of the capture coefficients. As in the case $m = 1$, the usually postulated scaling holds only when s is far enough from the most representative size (i.e. on the longest left tail of the SDs) and in the limit of infinitely long growth time or infinitely high diffusivity.

II. RATE EQUATIONS OF IRREVERSIBLE GROWTH

In modeling the time-dependent concentrations $n_s(t)$ of the immobile 2D or 3D clusters A_s consisting of s monomers (size s for brevity), we assume that the clusters are fed by the mobile monomers A_1 that have the diffusion coefficient D, arrive to the system at a time-independent rate I, and "desorb" with the characteristic time t_A. We neglect the decay of clusters on the timescale of interest, in which case the cluster growth proceeds irreversibly: $A_s + A_1 \rightarrow A_{s+1}$ for $s = 1,2,3\ldots$. The corresponding growth rates are given by $D\sigma_s$, with σ_s as the corresponding capture coefficients. Of course, for 3D systems, the capture coefficient should be proportional to a certain characteristic length from dimensional considerations. To write down the REs in the dimensionless form and to reduce the number of control parameters, we introduce the effective "diffusion length" $\lambda = \sqrt{\sigma_1 D t_A}$, the dimensionless time $\tau = t/t_A$, and the normalized concentrations $f_s = \lambda^2 n_s$ for all $s = 1,2,3\ldots$ including monomers.

The discrete REs describing the time evolution of the SD are given by [1–24]

$$\frac{df_1}{d\tau} = \nu - f_1 - 2f_1^2 - f_1\sum_{s=2}^{\infty} k_s f_s, \tag{1}$$

$$\frac{df_s}{d\tau} = f_1(k_{s-1}f_{s-1} - k_s f_s), \quad s = 2,3,4\ldots, \tag{2}$$

with

$$k_s = \frac{\sigma_s}{\sigma_1}, \tag{3}$$

as the effective dimensionless capture coefficients. The control parameter

$$\nu = \lambda^2 I t_A = \sigma_1 D I t_A^2 \tag{4}$$

has a clear meaning of the number of monomers arriving due to the influx I onto the area (or into the volume) $\lambda^2 = \sigma_1 D t_A$ during the lifetime t_A. Equation (1) shows that the concentration of free monomers changes due to the influx, sink, and monomer consumption by the growing clusters, where the dimer formation requires two monomers. The prefactors in the desorption $(-f_1)$ and the dimerization $(-f_1^2)$ terms are the same due to the specific choice of the effective diffusion length which contains σ_1. The chain of Eq. (2) shows that the concentration f_s for each $s \geqslant 2$ increases when monomers attach to $s-1$-mers and decreases when monomers attach to s-mers. These equations should be solved with zero initial conditions $f_s(0) = 0$ for all $s = 1,2,3\ldots$ corresponding to the beginning of the growth process at $\tau = 0$.

Let us introduce the total number (or the density) of all immobile clusters F and the total number of monomers in all immobile clusters G (both normalized by multiplying the corresponding dimensional values to λ^2) by definitions

$$F = \sum_{s=2}^{\infty} f_s; \quad G = \sum_{s=2}^{\infty} s f_s. \tag{5}$$

In the 2D case, G has the meaning of the dimensionless surface coverage. As follows from Eqs. (1) and (2), the cluster density changes in time only by dimerization, while the total number of monomers in the system changes only due to the external fluxes

$$\frac{dF}{d\tau} = f_1^2, \tag{6}$$

$$\frac{d}{d\tau}(f_1 + G) = \nu - f_1. \tag{7}$$

Very importantly, Eq. (6) shows that the nucleation rate in the irreversible growth model equals f_1^2 because nucleation occurs whenever two mobile monomers meet. This is distinctly different from classical nucleation theory [23,25–32] where the Zeldovich nucleation rate $dF/d\tau = J$ is a steep exponential function of supersaturation $\zeta = f_1/f_{\rm eq} - 1$, with $f_{\rm eq}$ as the equilibrium monomer concentration at a given temperature.

III. SIZE-INDEPENDENT CAPTURE COEFFICIENTS

We first consider the simplest case of size-independent capture coefficients $k_s = 1$ for all $s = 1,2,3\ldots$. Since $\sum_{s=2}^{\infty} k_s f_s = \sum_{s=2}^{\infty} f_s = F$, Eqs. (1) and (6) now constitute the closed system for the determination of f_1 and F

$$\frac{df_1}{d\tau} = \nu - f_1 - 2f_1^2 - f_1 F, \tag{8}$$

$$\frac{dF}{d\tau} = f_1^2, \tag{9}$$

with $f_1(\tau = 0) = F(\tau = 0) = 0$, depending on the sole control parameter ν.

We now introduce the new time-dependent variable $z \equiv s_*$ instead of time τ by definition

$$\frac{dz}{d\tau} = f_1, \quad z(\tau = 0) = 0. \tag{10}$$

Since all the growth rates in Eq. (2) now equal f_1 and are s independent, the physical meaning of the z variable is very simple: it corresponds to the right boundary of the SD (i.e. to the maximum possible size of clusters having emerged at $\tau = 0$) in the deterministic limit [23,26–28] where the SD shape is not affected by kinetic fluctuations [30]. This will be important in what follows.

Equations (2) for the cluster concentrations become linear in terms of the z variable

$$\frac{df_s}{dz} = f_{s-1} - f_s, \quad s = 2,3.4\ldots \tag{11}$$

The exact solutions to this system are easily obtained by implying the generating function for concentrations, as in Refs. [5,35]

$$f_{s+2}(z) = \frac{1}{s!}\int_0^z dx f_1(z-x)x^s e^{-x}, \quad s = 0,1,2\ldots \tag{12}$$

The monomer concentration f_1 should be obtained as a function of τ from Eqs. (8) and (9) and then inverted as a function of z by means of Eq. (10).

Graphs in Fig. 1 show the normalized monomer concentration $f_1/\nu^{1/3}$ and the island density $F/\nu^{2/3}$ as functions of the dimensionless time τ at different ν [obtained from numerically solving Eqs. (8) and (9)], compared to their large time asymptotes $f_1(\tau)/\nu^{1/3} = (3\tau)^{-1/3}$ and $F(\tau)/\nu^{2/3} = (3\tau)^{1/3}$ (see the asymptotic analysis given below). The discrete concentrations of differently sized clusters, calculated by means of Eqs. (12), are shown by dots in Fig. 2 for different z at the fixed ν and vice versa. These results demonstrate the two major properties. First, the monomer concentration reaches its maximum (which is noticeably smaller than ν) soon after the beginning of deposition at $\nu \gg 1$ as in complete condensation regime with negligible desorption [3]. In contrast, the incomplete condensation regime at $\nu \ll 1$ relates to the saturation of f_1 at $f_{1,\,\rm max} \cong \nu$, followed by a very slow regression for longer growth times [3,38]. The cluster density increases faster for larger ν. The asymptotic stage (corresponding to the dashed curves in Fig. 1) is reached almost immediately after passing the maximum of the monomer concentration at large enough ν, as in Ref. [5]. Second and more important, the SDs shown in Fig. 2 feature the shapes that are very similar to the f_1 shapes in Fig. 1, inverted in such a way that the time moment $\tau = 0$ corresponds to the maximum size present in the SDs. Indeed, the SDs decay very abruptly after passing their maxima, with a much slower regression toward smaller s. This observation

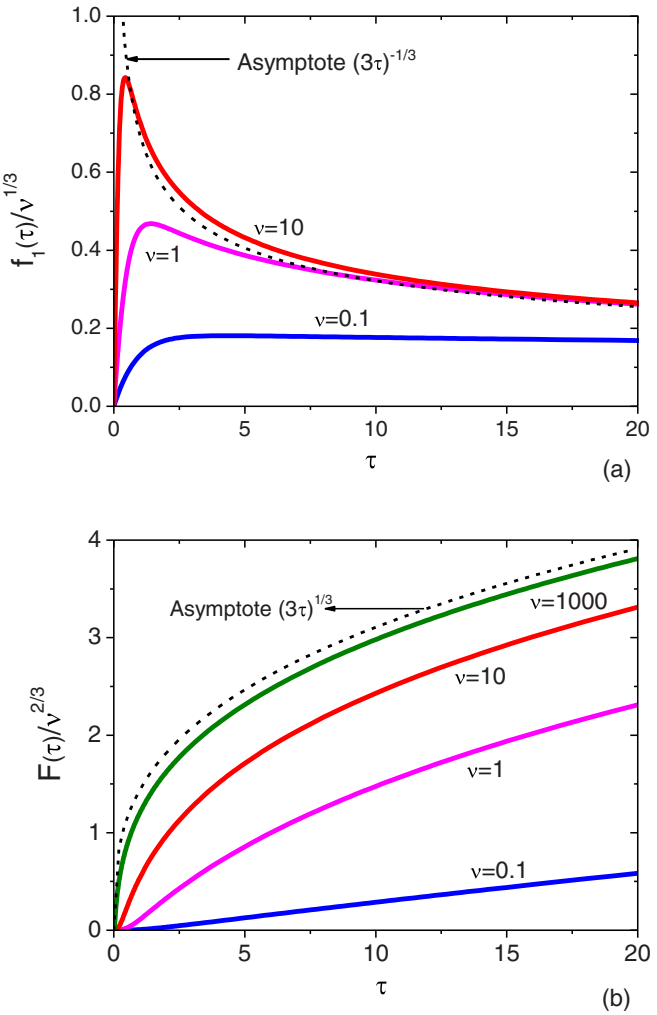

FIG. 1. (Color online) Graphs of (a) the normalized monomer concentration $f_1/\nu^{1/3}$ and (b) cluster density $F/\nu^{2/3}$ versus dimensionless time τ at different ν, compared to the asymptotic solutions (the dotted lines). The asymptotic stage is established very quickly for large ν, which is the regime with negligible desorption and at high diffusivity.

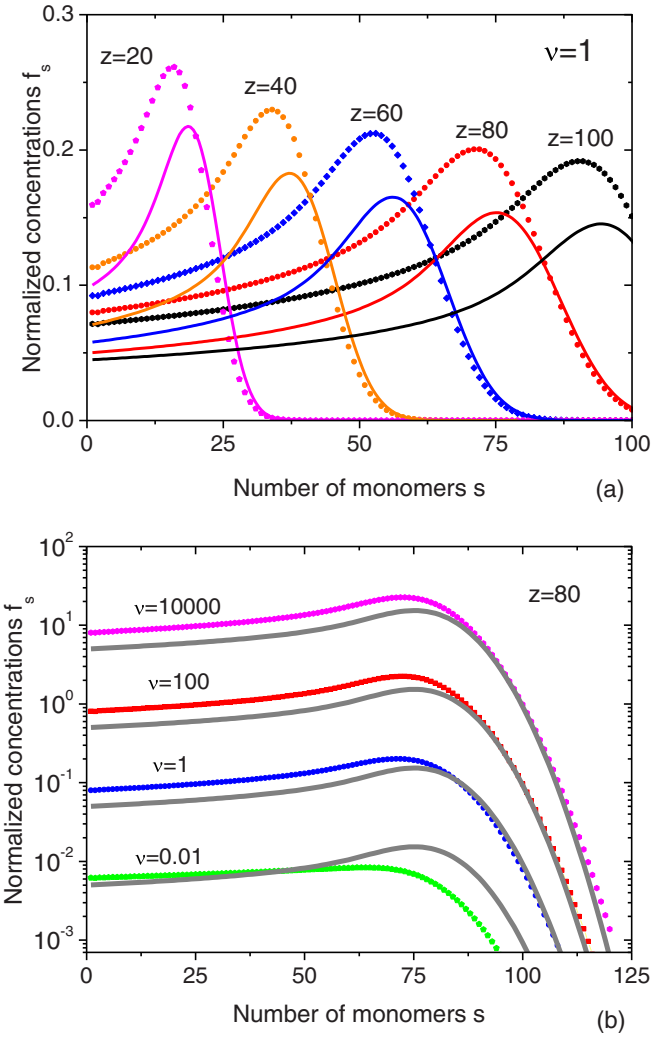

FIG. 2. (Color online) Size distributions at (a) fixed $\nu = 1$ and different z and at (b) fixed $z = 80$ and different ν. The dots show the discrete SDs and the solid lines represent the continuum SDs obtained from Eqs. (16) and (17). The continuum approximation works better for larger z and ν.

is fundamental for understanding the SD shapes in general, as will be discussed shortly.

We now consider the behavior of the exact solution given by Eq. (12) at large z. From Eq. (8), at small enough f_1, one obtains the asymptotic behavior of the monomer concentration in the form $f_1 \cong \nu/F$. Using this in Eqs. (9) and (10), we arrive at the well-known results [5,23]

$$F \cong (3\nu^2\tau)^{1/3}; \quad f_1 \cong \left(\frac{\nu}{3\tau}\right)^{1/3}; \quad z \cong \frac{\nu^{1/3}}{2}(3\tau)^{2/3}, \qquad (13)$$

showing that the cluster density scales with time as $\tau^{1/3}$ while the monomer concentration decreases as $\tau^{-1/3}$. Using the last two equations, we can invert f_1 as a function of z

$$f_1 \cong \left(\frac{\nu}{2z}\right)^{1/2}. \qquad (14)$$

The limit of high diffusivity and negligible desorption is the particular case of Eqs. (13). Indeed, returning to the dimensional island density $N = F/\lambda^2$ and the monomer concentration $n_1 = f_1/\lambda^2$, using Eq. (4) for ν and $t = t_A\tau$, we get the well-known asymptotic behavior [5,15,23]: $N \cong [(3I^2t)/(\sigma_1 D)]^{1/3}$ and $n_1 \cong [I/(3\sigma_1^2 D^2 t)]^{1/3}$. The desorption time t_A does not enter these expressions. Therefore, systems with desorption and arbitrary diffusivities show the same limiting behavior at long growth times as systems without desorption at large diffusivities and finite growth times. Equation (13) for z yields $z \sim (DI)^{1/3}t^{2/3}$, hence the z value must be much larger than one in both cases.

Substitution of Eq. (14) into Eq. (12) yields

$$f_{s+2}(z) = \left(\frac{\nu}{2}\right)^{1/2} \frac{1}{s!} \int_0^z dx \frac{x^s e^{-x}}{(z-x)^{1/2}}. \qquad (15)$$

Strictly speaking, this equation is not valid in the neighborhood of z because the monomer concentration near $\tau = 0$ is not described by its large z asymptote. However, one can assume that the abrupt right tail of the SD is resumed

due to the rapidly decreasing Gaussian exponent under the integral. The continuum representation of Eq. (15) at $s \gg 1$ and $z \gg 1$ is easily obtained by applying the Stirling formula $s! \cong (2\pi s)^{1/2}\exp(s\ln s - s)$ and presenting the function under the integral as $x^s\exp(-x) = \exp(s\ln x - x) \cong \exp(s\ln s - s)\exp[-(s-x)^2/(2s)]$. This yields the result of Bartelt and Evans [5], rewritten in terms of the z variable

$$f(s,z) \cong \left(\frac{\nu}{2\pi}\right)^{1/2} \frac{1}{(2z)^{1/4}} \varphi\left(\frac{s-z}{\sqrt{2z}}\right), \tag{16}$$

where the function $\varphi(p)$ is defined as

$$\varphi(p) = \int_p^\infty dx \frac{e^{-x^2}}{(x-p)^{1/2}} = e^{-p^2} \int_0^\infty dy \frac{e^{-y^2-2py}}{y^{1/2}}. \tag{17}$$

It is evident that $\varphi(p)$ is continuous and has continuous derivatives at $p = 0$.

This SD reaches its maximum slightly to the left from the point $s = z$, showing that the z value is only slightly larger than the most representative cluster size in the SD. The spectrum has the characteristic width $(2z)^{1/2}$ near the maximum and decreases as a power law function at $z - s \gg z^{1/2}$ and exponentially at $s - z \gg z^{1/2}$. These properties follow from

$$f(s,z) \cong \nu^{1/2} \begin{cases} \frac{1}{[2(z-s)]^{1/2}}, & z - s \gg \sqrt{2z} \\ \frac{\Gamma(\frac{1}{4})}{2^{7/4}\pi^{1/2}} \frac{1}{z^{1/4}}, & s = z \\ \frac{1}{2(s-z)^{1/2}} e^{-\frac{(s-z)^2}{2z}}, & s - z \gg \sqrt{2z} \end{cases}. \tag{18}$$

The comparison of the discrete and continuum SDs shown in Fig. 2 demonstrates that Eqs. (16) and (17) provide a reasonable fit to the discrete SDs at large ν (i.e. in the regime of complete condensation) and for large z, while at $\nu = 1$, the shape of the discrete SD is resumed with a more noticeable downward shift.

It is clear that the continuum SD given by Eq. (16) already has the time-invariant "scaling" form

$$\frac{f(s,z)}{\mu\nu^{1/2}} z^{1/4} = \varphi\left(\frac{s-z}{\sqrt{2z}}\right), \tag{19}$$

where $\mu = 1/(2^{3/4}\pi^{1/2})$ is the constant and φ is the unique, time-invariant function of its variable. More precisely, scaling in the general case should be considered as z invariance, where large z relates to either long growth times or high diffusivities as discussed above. This invariance is demonstrated in Fig. 3. When normalized to $f_1(z)$, this continuum SD is not a z-invariant function of the unique variable s/z, as suggested, e.g. in Refs. [5,6]. This property holds only for the long left tail of the spectrum at $z - s \gg \sqrt{2z}$ where, in view of Eqs. (18) and (14), $f(s,z)/f_1(z) \cong 1/(1-s/z)^{1/2}$. When $f_s(z)$ is divided by $f_1(z)$ [which tends to zero as $z^{-1/2}$ according to Eq. (14)], and is considered as a function of s/z in the formal limit $z \to \infty$ (relating to either $\tau \to \infty$ or $\nu \to \infty$ at finite τ), the perfectly continuum physical spectrum indeed acquires a singularity at $s = z$

$$\frac{f(s,z)}{f_1(z)} \cong \begin{cases} \frac{1}{(1-\frac{s}{z})^{1/2}}, & 1 - \frac{s}{z} \gg z^{-1/2} \\ \frac{\Gamma(\frac{1}{4})}{2^{5/4}\pi^{1/2}} z^{1/4}, & s = z \\ \frac{1}{2^{1/2}(\frac{s}{z}-1)^{1/2}} e^{-(z/2)(s/z-1)^2}, & \frac{s}{z} - 1 \gg z^{-1/2} \end{cases}, \tag{20}$$

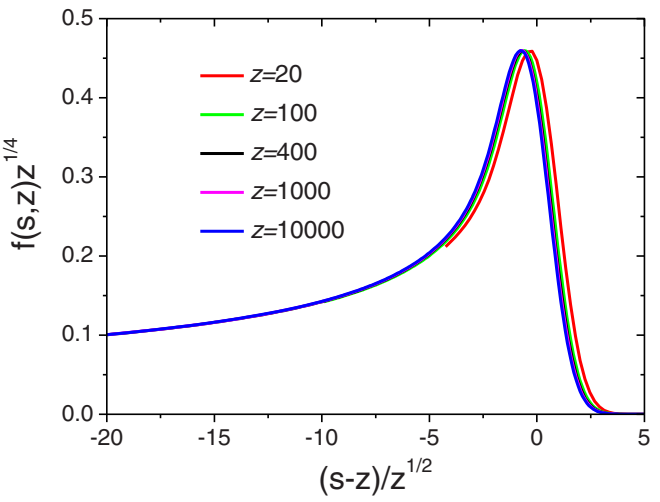

FIG. 3. (Color online) Collapse of the $f(s,z)z^{1/4}$ function to the unique value $\varphi[(s-z)/z^{1/2}]$ ($\nu = 1$). The curves at $z \geqslant 100$ cannot be distinguished.

which is exactly the result of Ref. [5]. This property is demonstrated in Fig. 4. Of course, since the average size $\langle s\rangle$ is proportional to z at large z (we will show later that $\langle s\rangle \cong (2/3)z$ in this particular case), the difference between s/z and $s/\langle s\rangle$ is just a multiplying factor and therefore is inessential for scaling.

IV. GROWTH RATES

Likewise in Ref. [30], we now turn to the analysis of different growth systems in the continuum limit $s \gg 1$ to see the possible dependences of the capture coefficients (or the growth rates) k_s on s. The latter are assumed to be dictated by the space dimensions, geometries, and mechanisms of material transport into an isolated cluster. Such an analysis is restricted to situations described within the mean field approach, i.e. neglecting the dependence of k_s on the coverage, island separation, concentrations, etc. [17,18]. We start with a

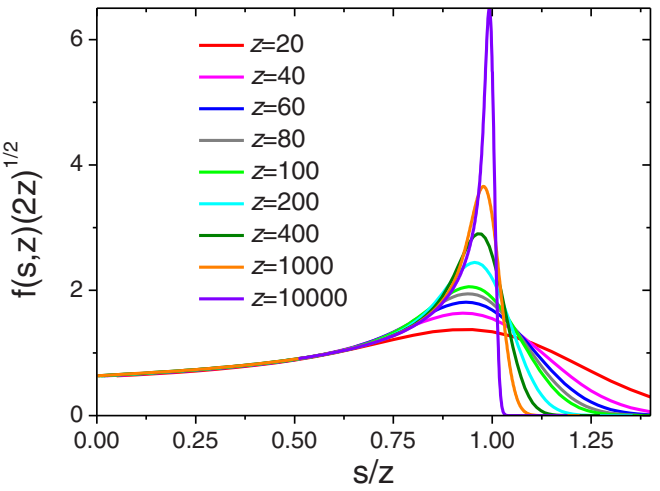

FIG. 4. (Color online) Collapse of the $f(s,z)(2z)^{1/2}$ to a nonanalytic function of s/z demonstrating the absence of z invariance in these variables ($\nu = 1$).

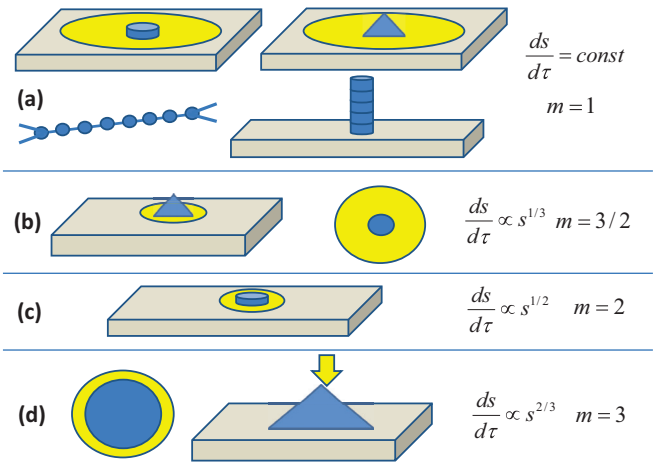

FIG. 5. (Color online) Schematics of different growth regimes yielding the power-law size dependences of the capture coefficients $k_s \propto s^{(m-1)/m}$ with $m = 1$, 3/2, 2, and 3. Yellow areas show the feeding zones of the clusters.

2D island growing in the diffusion regime where the effective diffusion length λ is much larger than the linear island size R. In this case, the islands consume adatoms from the entire diffusion ring $\pi\lambda^2$ irrespective of their size. With neglect of a minor logarithmic correction [13,23], the growth rate $ds/d\tau$ is independent of s. This yields $k_s \cong 1$, i.e. the case considered in the previous section. The same size independence holds for 3D surface islands growing in the diffusion regime. Other examples of s-independent capture coefficients include 1D linear chains in 3D space which can attach monomers only from their ends [24] and freestanding 1D "nanowires" growing perpendicular to the substrate by surface diffusion [23] [Fig. 5(a)]. Of course, the capture coefficients should also be size independent in the case of highly anisotropic 1D surface diffusion, e.g. along the steps [5].

When a 3D island with a fixed shape is fed from the adatom "sea" on a substrate surface in the ballistic regime such that the adatom diffusion length is much smaller than the radius of the island base R, the growth rate $ds/d\tau$ is proportional to R or $s^{1/3}$. This is also the case when, rather than from the adatom sea, 3D surface islands are fed from a strained wetting layer [23]. The same growth law applies to 3D clusters in 3D vapor environments in the diffusion regime. These systems are thus characterized by the capture coefficients $k_s \propto s^{1/3}$ [Fig. 5(b)]. For a 2D island growing in the ballistic regime at $\lambda \ll R$ [36], the growth rate is proportional to its perimeter, yielding $k_s \propto s^{1/2}$ [Fig. 5(c)]. Finally, when a 3D cluster grows in the ballistic regime from a 3D environment, the growth rate is proportional to the droplet surface area, i.e. $k_s \propto s^{2/3}$. The same dependence applies when a 3D droplet or island is seated on a substrate surface [Fig. 5(d)]. We note that in 3D systems as well as for vertical nanowires growing from a substrate, the coverage is usually very low, which justifies the use of RE approach for much longer times compared to 2D surface islands extending laterally.

It is seen that the capture coefficients of sufficiently large clusters ($s \gg 1$) feature the power law dependence on s which can be presented as

$$k_s = ms^{(m-1)/m}, \tag{21}$$

with the "growth index" $m = 1$, 3/2, 2, and 3 in the typical cases shown in Fig. 5. The growth rates $ds/d\tau$ thus equal $k_s f_1$, where f_1 is an analogue of supersaturation [23,25–33] in irreversible growth. Below in this paper, we will use Eq. (21) with arbitrary m between 1 and 3. However, generalization of our results to a more complex dependence $k_s = \phi(s)$ is rather straightforward. The mean field REs (without desorption and in the limit of large ratios of diffusion constant over deposition rate) with the power-law size dependence of the capture coefficients $\sigma_s = s^p$ with $0 \leqslant p < 1/2$ were studied earlier by Vvedensky [15]. In our notations, $p = 1 - 1/m$ and hence the Vvedensky solution corresponds to $m < 2$. It is important that the power-law k_s is itself a scaling function of s.

V. SIZE-DEPENDENT CAPTURE COEFFICIENTS: SOLUTIONS FOR CONTINUUM SIZE DISTRIBUTION

Introducing the z variable according to Eq. (10), the discrete REs given by Eq. (2) take the form

$$\frac{df_s}{dz} = k_{s-1}f_{s-1} - k_s f_s. \tag{22}$$

Continuum RE at $s \gg 1$ is obtained simply by expanding the $k_{s-1}f_{s-1}$ near s and leaving only the first and the second derivatives with respect to size

$$\frac{\partial f(s,z)}{\partial z} = -\frac{\partial}{\partial s}\left\{k_s f(s,t) - \frac{1}{2}\frac{\partial}{\partial s}[k_s f(s,z)]\right\}. \tag{23}$$

This kinetic equation is of the Fokker-Plank type, where the term with the first derivative describes the regular growth (ds/dz) at the rate k_s, while the second derivative stands for kinetic fluctuations. In what follows, we apply Eq. (21) for k_s uniformly for all $s \gg 1$. As usual in nucleation theory [23,26,27,30–32], we eliminate the trivial deformation of the SD due to the size dependence of the regular growth rate by introducing the new "invariant size" ρ by definition

$$\rho = s^{1/m}. \tag{24}$$

Obviously, $d\rho/dz = (d\rho/ds)(ds/dz) = (d\rho/ds)k_s = 1$, while in terms of τ, Eqs. (10) and (24) yield $d\rho/d\tau = dz/d\tau = f_1$, i.e. differently sized clusters now grow at exactly the same rate. For arbitrary homogeneous s dependence of the capture coefficients $k_s = \phi(s)$, the invariant size would be defined as

$$\rho = \int_0^s \frac{ds'}{\phi(s')}. \tag{25}$$

The new continuum SD in terms of the ρ variable should be introduced as

$$f(s,z)ds = g(\rho,z)d\rho, \tag{26}$$

so that the number of clusters in the intervals from s to $s + ds$ and from ρ and $\rho + d\rho$ is preserved.

From Eqs. (24) and (26), the continuum RE given by Eq. (23) in terms of the invariant size takes the form

$$\frac{\partial g(\rho,z)}{\partial z} = -\frac{\partial}{\partial \rho}\left\{ g(\rho,z) - \frac{\partial}{\partial \rho}\left[\frac{g(\rho,z)}{2m\rho^{m-1}} \right] \right\}. \tag{27}$$

The cluster density and the total number of monomers in all clusters in the continuum approximation are defined as

$$F(z) = \int_0^\infty d\rho g(\rho,z); \quad G(z) = \int_0^\infty d\rho \rho^m g(\rho,z), \tag{28}$$

where we use Eq. (26) and $s = \rho^m$. Using the continuum size distribution $g(\rho,z)$, one can introduce the averages of ρ^n by definition

$$\langle \rho^n \rangle = \frac{\int_0^\infty d\rho \rho^n g(\rho,z)}{\int_0^\infty d\rho g(\rho,z)}, \tag{29}$$

for arbitrary n. In particular, this yields

$$G = F\langle \rho^m \rangle. \tag{30}$$

As shown in Ref. [30], the Green function $g_0(\rho,z)$ of Eq. (27) describing the evolution of the SD from the point source $g(\rho,z=0) = \delta(\rho)$ can be approximated as

$$\begin{aligned} g_0(\rho,z) &= \frac{1}{\sqrt{2\pi\psi(z)}} \exp\left[-\frac{(\rho - z)^2}{2\psi(z)} \right], \\ \psi(z) &= \frac{z^{2-m}}{m(2-m)}, \quad m < 2, \end{aligned} \tag{31}$$

and

$$g_0(\rho,z) = \delta(\rho - z), \quad m \geqslant 2. \tag{32}$$

These results show that the SDs are broadened by the kinetic fluctuations at $m < 2$, while at $m \geqslant 2$, the SDs are not affected by fluctuations and remain purely deterministic. For $m < 2$, the dispersion of the SDs increases as a power law function of z. The threshold value of the growth index $m = 2$ corresponds to an almost negligible logarithmic broadening. The corrections to Eq. (31) asymptotically tend to zero at large z as $\sqrt{2\psi(z)}/z \sim z^{-m/2}$. The spectrum width either stays constant as growth proceeds (at $m \geqslant 2$) or increases more slowly than z (at $m < 2$). It is also seen that, in view of $\sqrt{2\psi(z)}/z \ll 1$, one can swap the variables z and ρ in the dispersion ψ in Eq. (31) by writing $\psi(z) \cong \psi(\rho)$ in the essential part of the spectrum $|\rho - z| \leqslant \sqrt{2\psi(z)}$.

Of course, the Green functions given by Eq. (31) at $m < 2$ and Eq. (32) at $m \geqslant 2$ meet neither initial nor boundary conditions of our problem. The initial condition in open systems is trivial: no clusters should be present in the system at $z = 0$. We also imply the condition that the SD vanishes at $\rho \to \infty$. The most important is the boundary condition at $\rho = 0$. In nucleation theory with the Zeldovich nucleation rate $dF/d\tau = J$, this boundary condition would imply that the stationary SD has the drift form $g(\rho = 0,z) = J/(d\rho/d\tau)$. This corresponds to the clusters with zero size emerging randomly at the rate J and surpassing the nucleation barrier with a size-independent velocity $d\rho/d\tau$ [23,24,26,27,29]. Since in our case $J = f_1^2$ and $d\rho/d\tau = f_1$, a similar boundary condition applies, i.e. $g(\rho = 0,z) = f_1(z)$. Rather than a formal limit for the continuum SD at $\rho \to 0$ that matches the monomer concentration at a given z, this boundary condition should be treated as the self-consistency criterion for irreversible growth with the quadratic dependence of the nucleation rate on the monomer concentration. Therefore, the relevant set of the initial and boundary conditions to Eq. (27) is given by

$$g(\rho,z=0) = 0; \quad g(\rho = \infty,z) = 0; \quad g(\rho = 0,z) = f_1(z). \tag{33}$$

The unknown $f_1(z)$ should now be obtained from the continuum equations following from Eqs. (1), (6), (10), (21), (24), and (29)

$$\frac{df_1}{d\tau} = f_1 \frac{df_1}{dz} = \nu - f_1 - m f_1 F \langle \rho^{m-1} \rangle; \quad \frac{dF}{dz} = f_1. \tag{34}$$

Whenever the SD is a solution to Eq. (27) with the boundary conditions given by Eqs. (33) and $f_1(z) \to 0$, it is easy to prove that

$$\frac{d}{dz}(F\langle \rho^m \rangle) = mF\langle \rho^{m-1} \rangle \tag{35}$$

for any m. Using this in the first equation in Eq. (34), we arrive at Eq. (7) with G given by Eq. (30). Integration of Eq. (7) in view of Eq. (10) yields the material balance in the form

$$f_1 + z + G = \nu\tau. \tag{36}$$

This formula shows simply that the monomers that have arrived to the system from a material influx by the moment of time τ can either remain as free monomers or desorb or get incorporated into the growing clusters.

Using the Green functions given by Eqs. (31) or (32), it is easy to construct the solutions to Eq. (27) which satisfy the required initial and boundary conditions defined by Eqs. (33)

$$\begin{aligned} g(\rho,z) &= \frac{1}{\sqrt{\pi}} \int_p^\infty dx e^{-x^2} f_1[\sqrt{2\psi(z)}(x - p)], \\ p &= \frac{\rho - z}{\sqrt{2\psi(z)}}, \quad m < 2, \end{aligned} \tag{37}$$

$$g(\rho,z) = f_1(z - \rho), \quad m \geqslant 2. \tag{38}$$

When $f_1(z)$ is given by Eq. (14), Eq. (37) is reduced to Eqs. (16) and (17) at $m = 1$ and $\rho = s$. The "deterministic" solution in Eq. (38) is the particular case of the SD obtained by Kuni for $m = 3$ [24], with the simplified stationary distribution f_1 in irreversible growth. Thus, the complete description of the SDs requires only the determination of the monomer concentration $f_1(z)$ at a given m. If wanted, these solutions can be inverted in terms of s and $\langle s \rangle$ by means Eqs. (24) and (26)

$$f(s,\langle s \rangle) = \frac{1}{ms^{1-1/m}} g(s^{1/m}, s_*^{1/m}) = \frac{1}{ms^{1-1/m}} g(s^{1/m}, \langle s \rangle^{1/m}) \tag{39}$$

for large s, because $\rho = s^{1/m}$ and $z = s_*^{1/m}$ is proportional to $\langle s \rangle^{1/m}$. Scaling properties of the obtained SDs at $z \to \infty$ will be discussed in detail in the foregoing sections. However, it is already clear that the appropriately normalized SDs should be the unique functions only of the combination of $(\rho - z)/\sqrt{2\psi(z)}$ at $m < 2$ or $(\rho - z)$ at $m \geqslant 2$, but not of ρ/z. Indeed, the simplest deterministic SD at $m \geqslant 2$ given

by Eq. (38) could be a scaling function in terms of variables $g(\rho,z)/f_1(z)$ and $\rho/z = (s/s_*)^{1/m} = \xi_m(s/\langle s\rangle)^{1/m}$ if and only if the $f_1(z)$ is a power law function of z. However, this cannot be the case because the monomer concentration increases with time at the beginning of growth and then decreases at the asymptotic stage [as in Fig. 1(a)]. Therefore, it cannot be presented as a single power law function of z: a combination of at least two power law functions is required to describe the $f_1(z)$ dependence with a maximum.

VI. ASYMPTOTIC ANALYSIS

Let us now consider the asymptotic growth stage at $f_1(z) \to 0$ which, for large enough values of ν, should hold for all but short times. The material balance given by Eq. (36) is now reduced to

$$G \cong \nu\tau, \tag{40}$$

i.e. the total volume of islands (or the coverage in 2D case) increasing linearly with time. As follows from Eqs. (37) and (38), the SDs either remain entirely deterministic (at $m \geqslant 2$) or broaden slower than the maximum deterministic size z (at $m < 2$). Therefore, at large enough z, the average value $\langle\rho^m\rangle = \langle s\rangle$ must be proportional to z^m with a negligible correction for the spectrum dispersion, i.e.

$$\langle\rho^m\rangle \cong B_m z^m, \tag{41}$$

with B_m independent of z.

We now search the asymptotic solution for $f_1(z)$ in the power-law form

$$f_1(z) \cong \frac{A_m}{z^\beta}, \tag{42}$$

where the power index β and the coefficient A_m need to be determined. Using this in Eqs. (10) and (34), Eq. (30) together with Eq. (41) and Eq. (40), respectively, yields the results

$$\beta = \frac{m}{2}; \quad A_m = \left[\frac{1}{B_m}\left(\frac{1-\frac{m}{2}}{1+\frac{m}{2}}\right)\nu\right]^{1/2}; \tag{43}$$

so that the A_m coefficients are expressed through B_m. On the other hand, applying Eq. (35) at $\langle\rho^m\rangle$ given by Eq. (41) leads to the recurrent formula

$$B_m = \frac{m}{1+m/2}B_{m-1}. \tag{44}$$

Since $B_0 = 1$ by definition, we are able to determine the B_m coefficients for integer m, in particular: $B_1 = B_2 = 2/3$, showing that the mean size $\langle\rho^m\rangle = \langle s\rangle$ equals two-thirds of the maximum deterministic size for $m = 1$ and 2. In the case of arbitrary fractional m, the B_m coefficients can be determined for a particular analytical SD [15] or numerically. Using Eq. (43) in Eqs. (42), (10), and (40) and the second equation in Eq. (34), we find the asymptotic growth laws in the form

$$f_1(z) \cong \frac{A_m}{z^{m/2}}; \quad F(z) \cong \frac{A_m}{1-\frac{m}{2}}z^{1-m/2};$$
$$G(z) \cong \frac{\nu}{A_m\left(1+\frac{m}{2}\right)}z^{1+m/2}; \quad \tau(z) \cong \frac{z^{1+m/2}}{A_m\left(1+\frac{m}{2}\right)}, \quad m < 2. \tag{45}$$

Here, the coefficients A_m are defined by the second equation in Eq. (43). These results are reduced to the corresponding Eqs. (13) and (14) in the particular case of $m = 1$.

We now note that Eqs. (45) is relevant only for $m < 2$ because the solution for the cluster density starts decreasing for $m > 2$ [the threshold value of $m = 2$ corresponds to only a logarithmic increase of $F(z)$]. This means that, rather than increasing infinitely at large z, the cluster density saturates at a certain maximum value $F_{\max}$ when $m > 2$. Repeating the above procedure at a time-independent $F_{\max}$ instead of an increasing $F(z)$, we arrive at a rather different limiting behavior

$$f_1(z) \cong \frac{C_m}{z^{m-1}}; \quad F(z) \cong F_{\max};$$
$$G(z) \cong F_{\max}z^m; \quad \tau(z) \cong \frac{z^m}{C_m m}, \quad m > 2. \tag{46}$$

Here, the C_m coefficients are expressed through $F_{\max}$ as

$$C_m = \frac{\nu}{m F_{\max}}, \tag{47}$$

while the value of $F_{\max}$ can be easily obtained for a particular SD at a given m, as will be discussed shortly.

VII. ANALYTICAL SIZE DISTRIBUTIONS AND SCALING PROPERTIES

With the obtained asymptotic behaviors, the simplified equation describing the evolution of the monomer concentration writes down as

$$\frac{df_1}{d\tau} = f_1\frac{df_1}{dz} \cong \nu - f_1 - f_1 \times \begin{cases} \left(\frac{\nu}{A_m}\right)z^{m/2}, & m < 2 \\ m F_{\max} z^{m-1}, & m > 2 \end{cases}, \tag{48}$$

with $f_1(0) = 0$. Here, we assume that the power law asymptotes for F and $\langle\rho^{m-1}\rangle$ can be applied uniformly from $\tau = 0$. Even with this simplification, Eq. (48) cannot be integrated analytically for arbitrary m, so we have to resort to some approximations. In the regime of complete condensation with $\nu \gg 1$, the relevant approximations are given by a combination of the two power-law functions that resume correctly the small time interpolation $f_1 \cong \nu\tau$ [where the $\tau(z)$ dependence is determined from either Eq. (45) or Eq. (46)] and the large z asymptotes. These approximate solutions are given by

$$f_1(z) \cong \nu^{1/2}\frac{a_m z^{1+m/2}}{1+b_m z^{1+m}}; \quad a_m = \left[\frac{B_m}{\left(1+\frac{m}{2}\right)\left(1-\frac{m}{2}\right)}\right]^{1/2};$$
$$b_m = \frac{B_m}{1-\frac{m}{2}}, \quad m < 2; \tag{49}$$

$$f_1(z) \cong \nu^{1/2} \frac{c_m z^m}{1 + d_m z^{2m-1}}; \qquad (50)$$

$$c_m = \frac{1}{m^{1/2}} \left[\int_0^\infty \frac{dx x^m}{1 + x^{2m-1}} \right]^{\frac{2m-1}{2(m+1)}}; \quad d_m = m c_m^2; \quad m > 2.$$

Here, the c_m coefficients at $m > 2$ were obtained from the normalization condition

$$F_{\max} = \int_0^\infty dz f_1(z). \qquad (51)$$

We have also extracted the large $\nu^{1/2}$ multiplying factor so that all other coefficients in these expressions for $f_1(z)$ are of the order of one.

Applying Eq. (49) with the substitution of $1 - m/2$ to 1 in the denominators of a_m and b_m (corresponding to the integration $\int dz/z = \ln z$) to the threshold case with $m = 2$ at $B_2 = 2/3$, we obtain the simple analytical expression

$$f_1(z) \cong \left(\frac{\nu}{3}\right)^{1/2} \frac{z^2}{1 + 2z^3/3}, \quad m = 2. \qquad (52)$$

Integration of this $f_1(z)$ leads to the logarithmic increase of the cluster density, as discussed earlier

$$F(z) \cong \frac{1}{2}\left(\frac{\nu}{3}\right)^{1/2} \ln\left(1 + \frac{2}{3}z^3\right), \quad m = 2. \qquad (53)$$

This completes the analytical description of $f_1(z)$ for all m. It is seen that the cluster density scales as $\nu^{1/2}$, which is also the case for $F_{\max}$ at $m > 2$.

The obtained analytical expressions were checked by comparing the results for $f_1(z)$ based on Eqs. (49), (50), or (52), the numerical solution of Eq. (48), and numerical integration of the initial discrete system given by Eqs. (1) and (2), for different m and ν. In particular, Fig. 6 shows the corresponding $f_1(z)$ at $\nu = 100$ for $m = 1$ and 3/2. It is seen that, while the maximum values of $f_1(z)$ cannot be fitted precisely by both approximations, the positions of the maxima as well as the large z asymptotes are described fairly well. Our calculations with different parameters reveal that the exact solution for $f_1(z)$ near the maximum (the red curves in Fig. 6) are always bound between the solution to Eq. (48) (the blue curves) and the analytical approximations (the black curves), with the discrepancy decreasing toward larger ν.

Based on the above analysis, we first consider the analytical SDs in the deterministic case $m \geqslant 2$, where the general solution is given by Eq. (38). Using Eqs. (50) and (52) for $f_1(z)$, one obtains

$$\frac{g(\rho,z)}{c_m \nu^{1/2}} \cong \begin{cases} \frac{(z-\rho)^m}{1+d_m(z-\rho)^{2m-1}}, & 0 \leqslant \rho \leqslant z \\ 0, & \rho > z \end{cases}, \quad m \geqslant 2, \qquad (54)$$

where $c_2 = 1/3^{1/2}$ and $d_2 = 2/3$ for $m = 2$. This solution shows the z-independent scaling for the SD expressed in terms of the $g/\nu^{1/2}$ and $\rho - z = s^{1/m} - s_*^{1/m}$ variables at large enough z because the right-hand side collapses to the unique, ν-independent function of $\rho - z$ after the SD at $\rho \to 0$ becomes close to zero.

When expressed in terms of the conventional scaling variables $g/f_{1\infty}$ and $\rho/z = (s/Z)^{1/m}$ [where $f_{1\infty}(z) = \nu^{1/2}(c_m/d_m z^{m-1}) = C_m/z^{m-1}$ is the asymptote of $f_1(z)$ at large z as given by the first equation in Eq. (46)], Eq. (54) takes the form

$$\frac{g(\rho,z)}{f_{1\infty}(z)} \cong \frac{(1-\rho/z)^m}{1/(d_m z^{2m-1}) + (1-\rho/z)^{2m-1}} \xrightarrow{z\to\infty} \frac{1}{(1-\rho/z)^{m-1}}. \qquad (55)$$

The formal limit at $z \to \infty$ gives the extreme case of the Bartelt-Evans singularity [5], where the purely deterministic function in the right-hand side tends to infinity at $\rho \to z$ and equals zero for all $\rho > z$ (because clusters with sizes larger than z cannot be present in the SD). As in the case of size-independent capture coefficients considered in Sec. III, this singularity arises because the SD near its maximum is not described by the same power-law function as on its left tail. Searching such a z-independent solution for all ρ is equivalent to assuming that the monomer concentration has

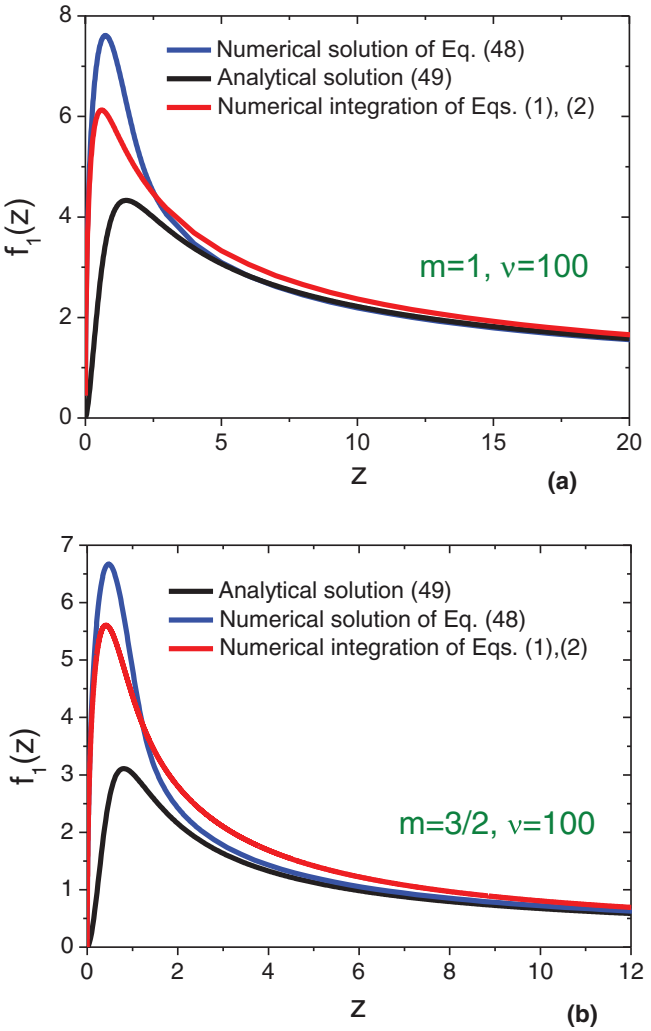

FIG. 6. (Color online) Monomer concentration f_1 as a function of z at the fixed $\nu = 100$, (a) $m = 1$ and (b) $m = 3/2$, obtained from different equations. In the case of $m = 3/2$, the coefficient $B_{3/2}$ equals approximately 0.8 from Eq. (41).

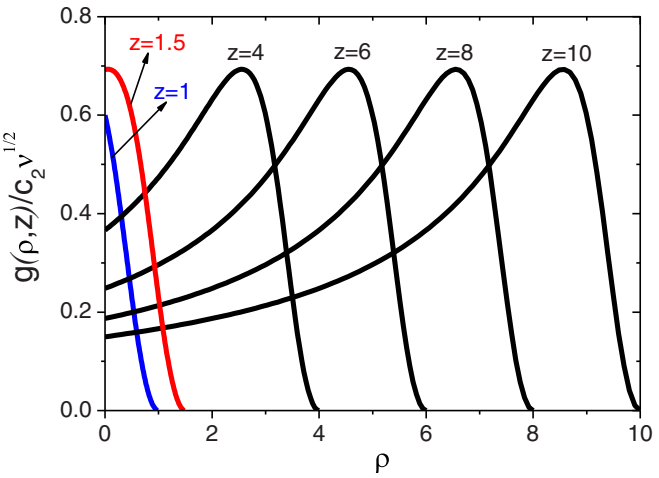

FIG. 7. (Color online) Deterministic SDs at $\nu = 100$ and $m = 2$ showing how the spectrum develops the maximum and then moves along the ρ axis without changing its shape as z increases.

never evolved from zero at the beginning of growth and has never reached its maximum but has been always decreasing as a power-law function of time, which is obviously not the case. The two different ways of presenting the SD at $m = 2$ are given in Figs. 7 and 8, showing a very similar behavior to the graphs in Figs. 3 and 4, although the capture coefficients are no longer size independent. It is also seen that that the SD given by Eq. (54) at finite z describes very well the so-called "nucleation catastrophe" [23], where the maximum of the spectrum develops and propagates to the right along the size axis as the growth time increases (Fig. 7). In terms of the $\rho - z$ variable, this situation is also described by the time-invariant distribution which is offcut by the condition $\rho \geqslant 0$, as in nucleation theory with the Zeldovich nucleation rate [26,27]. Compared to Fig. 3, the SDs shown in Fig. 7 are not affected by fluctuation-induced broadening, as is should be for $m = 2$.

In the case of $m < 2$, the SD is given by Eq. (37) which contains a rapidly decreasing Gaussian exponent under the integral. Due to this exponential decay, one can use the large z interpolation given by the first equation in Eq. (45) uniformly under the integral. This reduces Eq. (37) to

$$g(\rho,z) \cong \mu_m \nu^{1/2} \frac{1}{z^{(m/2)(1-m/2)}} \varphi_m(p); \tag{56}$$

$$p = \frac{\rho - z}{\sqrt{2\psi(z)}} = \left[m\left(1 - \frac{m}{2}\right)\right]^{1/2} \frac{(\rho - z)}{z^{1-m/2}}; \tag{57}$$

where the $\varphi_m(p)$ function is defined as

$$\varphi_m(p) = \int_p^\infty dx \frac{e^{-x^2}}{(x-p)^{m/2}}. \tag{58}$$

The coefficients μ_m are given by

$$\mu_m = \frac{m^{1/4}\left(1 - \frac{m}{2}\right)^{3/4}}{\left[\pi B_m\left(1 + \frac{m}{2}\right)\right]^{1/2}}. \tag{59}$$

Here, we use explicitly the z dependence of the dispersion, given by the second Eq. (31). Of course, this result is reduced to Eqs. (16) and (17) at $m = 1$.

This SD features the following asymptotic behaviors:

$$g(\rho,z) \cong \mu_m \nu^{1/2} \begin{cases} \frac{\pi^{1/2}}{[m(1-\frac{m}{2})]^{1/4}} \frac{1}{(z-\rho)^{m/2}}, & z - \rho \gg \sqrt{2\psi(z)} \\ \frac{\Gamma(\frac{1}{2}-\frac{m}{4})}{2} \frac{1}{z^{(m/2)(1-m/2)}}, & \rho = z \\ \frac{\gamma_m}{z^{(m-1)(1-m/2)}} \frac{\exp[-m(1-\frac{m}{2})\frac{(\rho-z)^2}{z^{2-m}}]}{(\rho-z)^{1-m/2}}, & \rho - z \gg \sqrt{2\psi(z)} \end{cases}, \tag{60}$$

i.e. the power-law form on the long left tail and the exponential Gaussian decay on the abrupt right tail. The refined scaling therefore holds in terms of the variables

$$\frac{g(\rho,z)}{\mu_m \nu^{1/2}} z^{(m/2)(1-m/2)} = \varphi_m\left\{\left[m\left(1 - \frac{m}{2}\right)\right]^{1/2} \frac{(\rho - z)}{z^{1-m/2}}\right\}, \tag{61}$$

where the right-hand side is the unique function of $(\rho - z)/z^{1-m/2}$. Such a scaling is distinctly different from the deterministic case [Eq. (54)] because the scaling variable contains the fluctuation-induced denominator $z^{1-m/2}$.

Vvedensky [15] obtained the following asymptotic solution for $m < 2$ in terms of the "natural" variables

$$f(\tilde{s},G) = Q_m \frac{G}{\langle s\rangle^2} \frac{1}{\tilde{s}^{1-1/m}(1 - \xi_m \tilde{s}^{1/m})^{m/2}}, \tag{62}$$

where G is the coverage, $\tilde{s} = s/\langle s\rangle$ and Q_m, ξ_m are the coefficients which depend on the growth index m. From Eqs. (43) and (45), our solution yields $G = C \times \nu^{1/2} z^{1+m/2}$ (where C is a constant) because A_m scales as $\nu^{1/2}$. Using Eq. (60) for the left tail of the SD and Eq. (39), we get

$$f = C \times \frac{G}{z^{1+m} s^{1-1/m}} \frac{1}{(1 - \frac{\rho}{z})^{m/2}}, \tag{63}$$

where the prefactor depends on m. The equivalence of Eqs. (62) and (63) follows upon the substitution $\rho = s^{1/m}$ according to Eq. (24) and $z = \langle s\rangle^{1/m}/\xi_m$. Furthermore, a more detailed analysis shows that the coefficients Q_m and ξ_m in the Vvedensky formula given by Eq. (62) and in our solution are exactly identical.

If normalized to the asymptotic $f_1(z)$ at large z as in Ref. [5], the SD becomes

$$\frac{g(\rho,z)}{f_1(z)} = C \times z^{m^2/4} \varphi_m\left(\frac{\rho - z}{\sqrt{2\psi(z)}}\right), \tag{64}$$

which gives the $z^{m^2/4}$ singularity at $z \to \infty$ for $\rho = z$. We saw this discontinuity earlier in Sec. III in the particular case $m = 1$. It is clear that the additional power index $m^2/4$ arises due

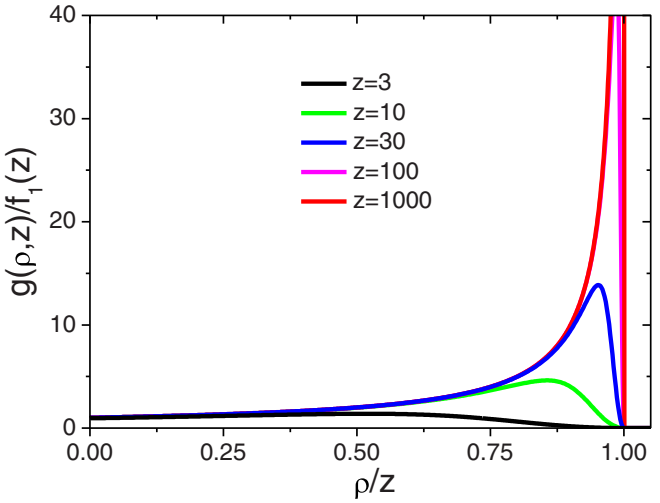

FIG. 8. (Color online) Same distribution as in Fig. 7 replotted in terms of the g/f_1 and ρ/z variables. The red line at $z = 1000$ gives the singular asymptote $1/(1-\rho/z)$ which is a good approximation at the left tails of the SDs for large enough z.

to kinetic fluctuations. As in the deterministic case, presenting the right-hand size of Eq. (64) in terms of the g/f_1 and ρ/z variables at $z \to \infty$ basically reduces the normalized SDs to their asymptote on the left tail

$$\frac{g(\rho,z)}{f_1(z)} = \begin{cases} \frac{C}{(1-\frac{\rho}{z})^{m/2}}, & \rho < z \\ 0, & \rho > z \end{cases}. \tag{65}$$

This is the Bartelt-Evans singularity which arises also in the case of arbitrary growth index m, as was demonstrated earlier in Ref. [15].

The obtained continuum SD is shown in Fig. 9 in the case $m = 3/2$, compared to the results of numerical integration of discrete REs given by Eqs. (10) to (12). The same continuum distribution expressed in the refined scaling variables defined by Eq. (61) is presented in Fig. 10, whereas Fig. 11 shows

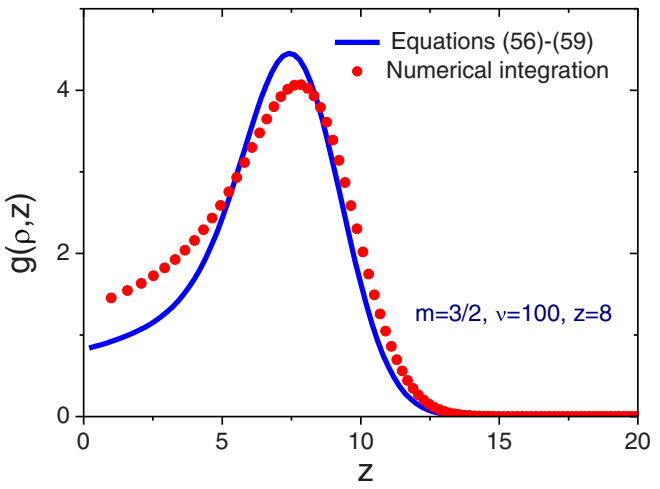

FIG. 9. (Color online) Size distributions at $m = 3/2$, $\nu = 100$, and $z = 8$, obtained from Eqs. (56) to (59) and from numerical integration of discrete Eqs. (10) to (12).

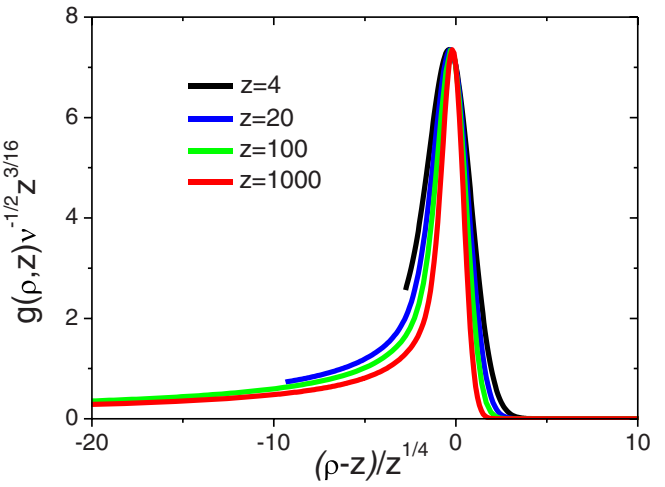

FIG. 10. (Color online) Continuum distribution at $m = 3/2$, $\nu = 100$, and different z, presented in terms of scaling variables defined by Eq. (61).

the SDs in the Bartelt-Evans coordinates. Qualitatively, the picture remains the same as in Figs. 3 and 4 and demonstrates that the z-independent scaling in terms of the g/f_1 and ρ/z variables cannot be resumed even when capture coefficients are size dependent. Our analysis also shows that the choice of the refined scaling variables at $m < 2$ must account for fluctuations described by the second derivative in the continuum RE.

In terms of the "natural" variables $f(s,s_*)$, where s_* is the maximum size in the deterministic limit, related to the average number of monomers in the clusters as $\langle s \rangle = B_m s_*$, our refined scaling has the form

$$\frac{m s^{1-1/m} f(s,s_*)}{c_m \nu^{1/2}} = C \times \frac{s^{1-1/m} f(s,s_*)}{G} s_* = \phi_m(s_*^{1/m} - s^{1/m}), \quad m \geqslant 2; \tag{66}$$

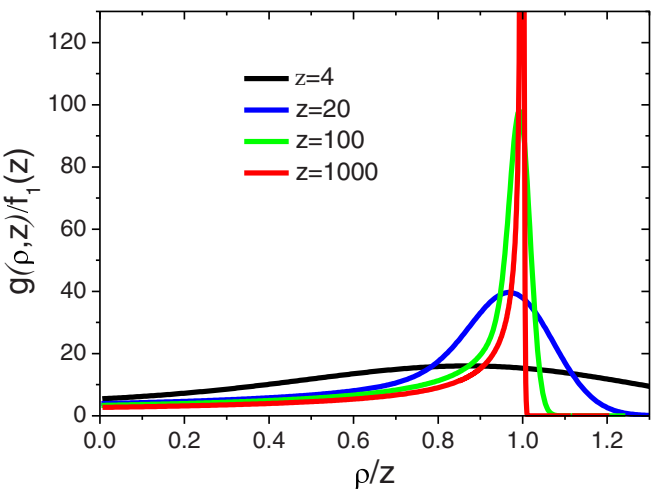

FIG. 11. (Color online) Same distribution as in Fig. 12 replotted in terms of the g/f_1 and ρ/z variables.

$$\frac{ms^{1-1/m}f(s,s_*)}{\mu_m \nu^{1/2}} s_*^{1/2-m/4} = C \times \frac{s^{1-1/m}f(s,s_*)}{G} s_*^{1+1/m-m/4} = \varphi_m\left(\frac{s_*^{1/m}-s^{1/m}}{s_*^{1/m-1/2}}\right), \quad 1 \leqslant m < 2; \tag{67}$$

Here, we use different formulations of scaling discussed previously [4,5,15,17,18–22], i.e. through s_* and $\nu \propto D$ or through s_* and the coverage G. The unique scaling functions in the right-hand sides are given by Eqs. (54) and (61), respectively, with $\rho = s^{1/m}$ and $z = s_*^{1/m}$. Very importantly, since both f and G are proportional to λ^2 in our normalization, the dependence on the control parameter ν and therefore of all the physical parameters (D, I, t_A) enters only the coverage $G(G \propto \nu^{1/2})$, while the scaling functions are independent of ν. The factor $s^{1-1/m}$ arises due to the size dependence of the capture coefficients and the deterministic deformation of the SDs caused by it. The cause of the factor $s_*^{1/m-1/2}$ in Eq. (67) is kinetic fluctuations. When the coverage G is introduced into the scaling expressions, the different power-law behaviors of the s_* factors is due to different dependences of $G(s_*)$ and the absence or presence of kinetic fluctuations at $m \geqslant 2$ or $m < 2$, respectively.

In the formal limit $z \to \infty$, which requires either infinite growth time or infinitely high diffusivity, Eqs. (66) and (67) can be reduced to the nonanalytic scaling functions of s/s_* according to

$$f\left(\frac{s}{s_*},s_*,G\right) = C \times \frac{G}{s_*^{3-2/m}} \frac{1}{\left(\frac{s}{s_*}\right)^{1-1/m}\left[1-\left(\frac{s}{s_*}\right)^{1/m}\right]^{m-1}}, \quad m \geqslant 2; \tag{68}$$

$$f\left(\frac{s}{s_*},s_*,G\right) = C \times \frac{G}{s_*^{2}} \frac{1}{\left(\frac{s}{s_*}\right)^{1-1/m}\left[1-\left(\frac{s}{s_*}\right)^{1/m}\right]^{m/2}}, \quad 1 \leqslant m < 2; \tag{69}$$

The constant prefactors depend on m and are easily deduced from the expressions given above. Equation (69) is identical to the Vvedensky solution [15], while Eq. (68) generalizes the latter to the case $m \geqslant 2$. The scaling functions of s/s_* in the right-hand sides are singular only at $s/s_* = 1$ for $m = 1$ and at the two points $s/s_* = 0$ and 1 for $m > 1$. Therefore, whenever the capture coefficient is an increasing power-law function of s, the s/s_* scaling acquires the singularity not only for large but also for small sizes. The functions given by Eqs. (68) and (69) are shown in Fig. 12 for different m.

Summarizing, we have included desorption into the REs for irreversible growth and constructed the corresponding analytical solutions for the SDs by using the z variable instead of time or coverage. It has been shown that the simplest case of the size-independent capture coefficients ($m = 1$) is affected by the purely Poissonian random broadening of the SD, which is in fact well known in general growth theory [39]. We have considered the size-dependent capture coefficients of the power-law form $ms^{(m-1)/m}$ and obtained the analytical

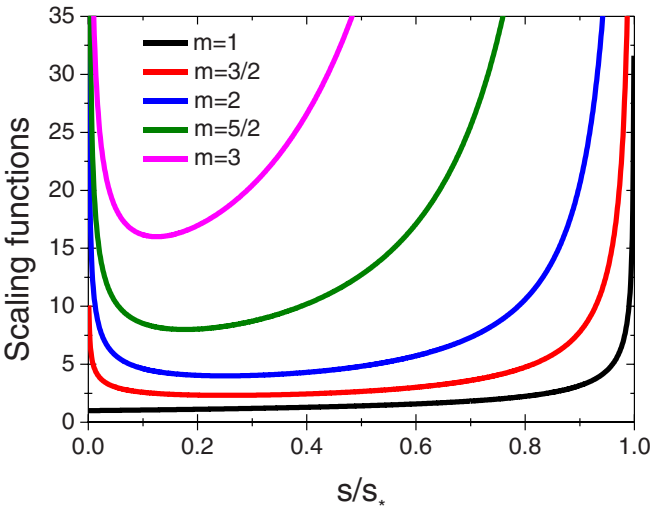

FIG. 12. (Color online) Scaling functions of s/s_* at different m.

solution for the SDs for arbitrary m. As in general nucleation theory with decay [30], the fluctuation-induced broadening of the SDs is present at $m < 2$ and absent at $m \geqslant 2$.

In any case, the appropriately normalized SDs feature the unique scaling shapes in terms of the correct variables and do not feature scaling for finite z if presented as functions of ρ/z. This property holds only for the long left tail of the SDs, i.e. for small enough clusters. In simple terms, it can be said that the SD shapes reflect the time dependence of the monomer concentration, which first rapidly increases and then slowly decreases with time. The SDs are obtained roughly by inverting the z-dependent $f_1(z)$ in terms of the $z - \rho$ variable, as has been known for a long time [26] in a more general case. This refined scaling gives a more detailed picture of the universal SD behaviors starting from the initial nucleation step up to infinite z and does not require the assumptions of large ratios of diffusion constant over deposition or desorption rate. In the formal limit $z \to \infty$, all the obtained SDs can be presented as nonanalytic scaling functions in terms of the ρ/z or s/s_* variable, as discussed earlier [4,5,15]. At $m = 1$, the scaling function is singular for large sizes [5], while at any $m > 1$, it acquires the second singularity for small sizes [15].

The main results regarding the refined scaling and the conventional scaling, converted into the "natural" variables, are given by Eqs. (66)–(69), respectively. In both cases, the dependence on the control parameter ν is contained only in the coverage G, while the universal scaling functions depend only on the growth index m.

Our results have been obtained based on the mean field RE approach. A careful analysis of the cooperative effects in the regimes with negligible desorption is required to investigate whether the refined scaling would be relevant also in this case. The obtained size distributions can be useful for modeling concrete systems, including those with very high diffusivity and in complete condensation regime, but also systems with high desorption rates. We now plan to investigate in more detail the regimes of incomplete condensation and to consider particular growth processes from the viewpoint of the obtained results. Another important generalization could be more complex multicomponent systems described within the

RE approach [40,41]. As a general conclusion, our analysis shows that the commonly believed scaling at finite growth times and diffusivities holds only at the long left tail of the SDs. The asymmetry of the SDs is due to the no-decay assumption and therefore is the most questionable among other approximations. Consequently, an interesting direction is including cluster decay for longer growth times, which would shorten the left tail and could change completely the scaling properties for smaller particles.

ACKNOWLEDGMENTS

This work was partially supported by different scientific programs of the Russian Academy of Sciences, a few grants of the Russian Foundation for Basic Research, contracts with the Russian Ministry of Education and Science, and the FP7 projects NANOEMBRACE and FUNPROB. N.V.S. gratefully acknowledges support from the Grant Council of President of the Russian Federation for young scientists.

[1] J. A. Venables, Philos. Mag. **27**, 697 (1973).
[2] S. Stoyanov and D. Kashchiev, Curr. Top. Mater. Sci. **7**, 69 (1981).
[3] A. Venables, G. D. T. Spiller, and M. Hanbucken, Rep. Prog. Phys. **47**, 399 (1984).
[4] T. Vicsek and F. Family, Phys. Rev. Lett. **52**, 1669 (1984).
[5] M. C. Bartelt and J. W. Evans, Phys. Rev. B **46**, 12675 (1992).
[6] M. C. Bartelt, M. C. Tringides, and J. W. Evans, Phys. Rev. B **47**, 13891 (1993).
[7] M. C. Bartelt and J. W. Evans, Phys. Rev. B **54**, R17359 (1996).
[8] J. W. Evans and M. C. Bartelt, Phys. Rev. B **63**, 235408 (2001).
[9] G. S. Bales and D. C. Chrzan, Phys. Rev. B **50**, 6057 (1994).
[10] G. S. Bales and A. Zangwill, Phys. Rev. B **55**, R1973 (1997).
[11] P. A. Mulheran and J. A. Blackman, Philos. Mag. Lett. **72**, 55 (1995).
[12] J. G. Amar and F. Family, Phys. Rev. Lett. **74**, 2066 (1995).
[13] P. Jensen, H. Larralde, and A. Pimpinelli, Phys. Rev. B **55**, 2556 (1997).
[14] F. G. Gibou, C. Ratsch, M. F. Gyure, S. Chen, and R. E. Caflisch, Phys. Rev. B **63**, 115401 (2001).
[15] D. D. Vvedensky, Phys. Rev. B **62**, 15435 (2000).
[16] M. Korner, M. Einax, and P. Maass, Phys. Rev. B **82**, 201401 (2010).
[17] M. Korner, M. Einax, and P. Maass, Phys. Rev. B **86**, 085403 (2012)
[18] J. W. Evans, P. A. Thiel, and M. C. Bartelt, Surf. Sci. Rep. **61**, 1 (2006).
[19] W. Dieterich, M. Einax, and P. Maass, Eur. Phys. J. Special Topics **161**, 151 (2008).
[20] C. Ratsch and J. A. Venables, J. Vac. Sci. Technol. A **21**, S96 (2003).
[21] H. Brune, Surf. Sci. Rep. **31**, 121 (1998).
[22] M. Einax, W. Dieterich, and P. Maass, Rev. Mod. Phys. **85**, 921 (2013).
[23] V. G. Dubrovskii, *Nucleation Theory and Growth of Nanostructures* (Springer, Heidelberg, New York, Dordrecht, London, 2014).
[24] V. G. Dubrovskii, N. V. Sibirev, I. E. Eliseev, S. Yu. Vyazmin, V. M. Boitsov, Yu. V. Natochin, and M. V. Dubina, J. Chem. Phys. **138**, 244906 (2013).
[25] D. Kashchiev, *Nucleation: Basic Theory with Applications* (Butterworth-Heinemann, Oxford, 2000).
[26] F. M. Kuni, Colloid J. USSR **46**, 791 (1984).
[27] F. M. Kuni, A. K. Shchekin, and A. P. Grinin, Phys. Usp. **171**, 345 (2001).
[28] S. A. Kukushkin and A. V. Osipov, Prog. Surf. Sci. **51**, 1 (1996).
[29] V. A. Shneidman, Phys. Rev. Lett. **101**, 205702 (2008).
[30] V. G. Dubrovskii, J. Chem. Phys. **131**, 164514 (2009).
[31] V. G. Dubrovskii and M. V. Nazarenko, J. Chem. Phys. **132**, 114507 (2010).
[32] V. G. Dubrovskii and M. V. Nazarenko, J. Chem. Phys. **132**, 114508 (2010).
[33] I. M. Lifshitz and V. V. Slyozov, J. Phys. Chem. Solids **19**, 35 (1961).
[34] J. A. D. Wattis and J. R. King, J. Phys. A: Math. Gen. **31**, 7169 (1998).
[35] J. R. King and J. A. D. Wattis, J. Phys. A: Math. Gen. **35**, 1357 (2002).
[36] T. Michely and J. Krug, *Islands, Mounds and Atoms: Patterns and Processes in Crystal Growth Far from Equilibrium* (Springer, Berlin, 2004).
[37] Y. W. Mo, J. Kleiner, M. B. Webb, and M. G. Lagally, Phys. Rev. Lett. **66**, 1998 (1991).
[38] V. G. Dubrovskii, Phys. Status Solidi B **171**, 345 (1992).
[39] V. G. Dubrovskii, Phys. Rev. B. **87**, 195426 (2013).
[40] M. Kotrla, J. Krug, and P. Smilauer, Phys. Rev. B **62**, 2889 (2000).
[41] M. Einax, S. Ziehm, W. Dieterich, and P. Maass, Phys. Rev. Lett. **99**, 016106 (2007).